Optical nanogap matrices for plasmonic enhancement applications

Stephen J. Bauman[a], Desalegn T. Debu[b], Avery M. Hill[b], Eric C. Novak[a,c], Douglas Natelson[d,e], Joseph B. Herzog[*,a,b,f]

[a]Microelectronics-Photonics Program, University of Arkansas, Fayetteville, AR, 72701, USA;
[b]Department of Physics, University. of Arkansas, Fayetteville, AR, 72701, USA;
[c]Department of Physics, Shippensburg University, Shippensburg, PA, 17257, USA;
[d]Department of Physics & Astronomy, Rice University, Houston, TX, 77005, USA;
[e]Department of Electrical & Computer Engineering , Rice University, Houston, TX, 77005, USA;
[f]Institute for Nanoscience and Engineering, University of Arkansas, Fayetteville, AR 72701, USA

ABSTRACT

Plasmonic structures can be used to enhance electromagnetic radiation, and nanoscale (<5 nm) gaps can increase this enhancement even further. Fabrication of these desired structures involves using a relatively new, previously developed self-aligned process to overcome typical electron beam lithography resolution limits. The resulting nanogap structures have been shown to exhibit enhanced optical emission. This technique enables the fabrication of a large-area two-dimensional matrix of such nanostructures which could prove useful for photovoltaics, plasmonically enhanced Raman spectroscopy, biosensing, and other optoelectronic applications. Computational electromagnetic simulations of the structures will prove useful for predicting behavior upon interaction with light and for experimental comparison.

Keywords: Plasmon, nanogap, sub-10nm nanofabrication, electron beam lithography (EBL), Plasmonic enhancement, optical enhancement, finite element method (FEM)

1. INTRODUCTION

A plasmon is the collective oscillation of electrons at the surface of a metal upon exposure to an electric field. The field of plasmonics studies the interaction of light, which has an oscillating electric field, with metal surfaces and the effects caused by these electron waves. There are an increasing number of plasmonically enhanced applications being studied to date. Arrays of metallic nanostructures are a large part of many efforts to utilize plasmonic enhancement across large surfaces.[1] Plasmonics have shown application in SERS and single molecule detection.[2,3] Plasmonics may be able to improve absorption in photovoltaic devices.[4] Some other studies involve Fano resonances of plasmonic devices,[5] metallic structures in conjunction with quantum dots,[6] as well as applications in nanoscopy and biosensing,[7] spasers,[8,9] and thermoplasmonics.[10–12]

Different methods are involved in fabrication of nanostructures capable of exhibiting plasmonic activity upon incident light emission. Due to the resolution limits of fabrication due to EBL proximity effects[13] and flaws with other techniques, new methods are being developed to allow necessary resolution of nanostructures. The present work focuses on fabrication of nanogaps on the order of less than 10 nm. Such gaps have been shown to exhibit electric field enhancement upon illumination.[2,3] The previously developed one dimensional self-aligned technique successfully demonstrates sub-5 nm gap fabrication.[2,14,15] Another method being studied for the production of sub-5 nm gaps is the helium focused ion beam method.[16]

Scaling up such fabrication techniques for the production of large area two-dimensional arrays of plasmonic nanostructures is crucial to many applications. Many methods capable of producing sufficiently small features do not prove to be efficient for production over large areas. Nanoskiving is one technique that involves a multi-step process for fabrication of nanoscale features across a large area.[17] The method described here is an extension of the previously mentioned one-dimensional self-aligned technique that allows for the same high resolution of nanogaps while allowing efficient production on a large two-dimensional scale.

[*] Email: jbherzog@uark.edu

Plasmonics: Metallic Nanostructures and Their Optical Properties XII, edited by Allan D. Boardman, Proc. of SPIE Vol. 9163, 91631A · © 2014 SPIE
CCC code: 0277-786X/14/$18 · doi: 10.1117/12.2061899

2. FABRICATION METHOD

The fabrication technique utilized to create plasmonic nanostructures in this work is the self-aligned process that has been previously developed and discussed.[14,15] It is a two-step process in which the resolution of the final deposition step relies on the initially fabricated structures. Electron beam lithography (EBL) was used to fabricate the initial pattern in PMMA on a silicon oxide wafer. Nanopattern Generation System (NPGS) software was used in conjunction with DesignCAD design software to create patterns to be written. The wafer was spin-coated with PMMA to prepare the sample for EBL. An accelerating voltage of 30 kV and a beam current around 10 pA on the FEI XL30 SEM were used during the writing process. NPGS was used to control beam dose, array parameters, dwell time, and other parameters during writing. The current resolution limit of this step for EBL in this work is around 100 nm, however, these are preliminary results and typically EBL can fabricate quality structures as small as 60 nm. After electron beam exposure, samples were then developed with 3:1 IPA:MIBK to remove the exposed areas of PMMA. Room temperature electron beam evaporation was used to deposit an adhesion layer of titanium (15 Å at 1 Å/s) then gold (150 Å at 2 Å/s), a silicon dioxide layer (15 Å at 0.3 Å/s), and chromium (150 Å at 1 Å/s), similar to previous work.[3,10] Once the vacuum chamber of the electron beam evaporator is vented, the chromium layer oxidizes, causing it to overhang the edges of the gold pattern as shown in Fig. 1a. This overhang was used as a shadow mask for the second EBL step.

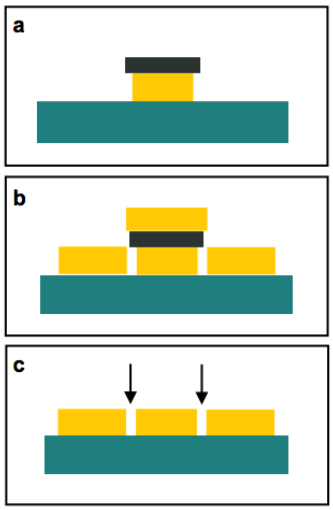

Figure 1. Self-aligned fabrication process. (a) Gold is patterned with a Cr layer using lithography. The Cr layer expands due to oxidation to overhang the Au layer. (b) Second Au deposition step. (c) Resulting structure when the chrome layer has been etched away.

The sample was spin-coated a second time with the same parameters and the second lithography and evaporation was performed. Due to the presence of the Cr oxide shadow mask, gold was not deposited under the Cr oxide during the second evaporation step. Instead only the areas beyond the edge are filled in during the second evaporation of gold. The result of the second evaporation step is shown in Fig. 1b. The Cr (gray) and SiO_2 (not shown) layers were etched away using Cr etchant, and buffered oxide etchant. The results are structures with the initial gold structure separated from the new one by a nanogap on all sides (Fig. 1c). The dimensions of the gap are well below the resolution limit of typical EBL fabrication.

3. FABRICATION RESULTS

The self-aligned fabrication technique has been previously shown to produce sub-10 nanometer gaps in one dimension.[14,15] The present work has expanded upon these previous results to demonstrate gaps in two dimensions. Different pattern configurations have been fabricated that exhibit gaps in a two-dimensional plane versus just a single linear gap for a given nanostructure. Gap size is on the order of 5-10 nm and is independent of the two-dimensional orientation. Thus the two-step process was successful in demonstrating 2D gap structures on the order of those exhibited in the 1D prior work.[3]

A large-area grid pattern array with many nanogaps is shown in Fig. 2. One advantage of this fabrication technique is the ability to mass-produce many nanogaps over a large area in parallel also having a large array allows for easier characterization or sensing applications.

The ability to fabricate these structures makes it easier to perform optical characterization tests that can be compared to FEM simulation results. With the initial fabrication results proving successful, the next step is to produce many structures over a large area and optimize the process to reduce errors. Because many plasmonic enhancement applications rely on tuning to specific optical wavelengths, the ability to precisely control gap and nanostructure dimensions is critical. This capability has been demonstrated for one dimensional gaps.[14] It will be important to reproduce this level of control in two dimensions.

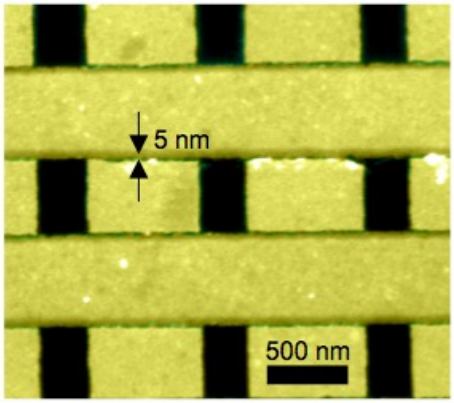

Figure 2. Colorized SEM images of self-aligned fabrication results: A large area nanowire grid pattern with nanogaps.

4. SIMULATIONS

Computational electromagnetic models were created with the COMSOL 4.4 radio frequency (RF) module, a program that uses the finite element method (FEM) to solve Maxwell's equations to simulate the electromagnetic response of nanoscale devices. The first set of models, shown in Figure 3, simulates the optical response of an infinitely long nanowire with rectangular cross-section. The cross sectional geometry of the infinitely long structure can be modeled in two dimensions as shown in Fig. 3a-b. Gold material properties are assigned to the nanostructure while an effective medium, n_{eff} =1.25, is applied to the surrounding environment to approximate the effect of the substrate.[3,10] An electromagnetic wave is incident on the device from a direction normal to the top surface. Since plasmonically enhanced devices attribute polarization dependent responses,[3] the wave is consistently polarized along the short axis of the device (transverse polarization).

Electromagnetic field distribution (EFD) is defined as E_{local}/E_0 where E_{local} is the local electric field at locations near the structure and E_0 is the incident electric field amplitude. Thus, the EFD calculated by the simulations is a unit-less value. The enhancement is simply the EFD squared, since the intensity of light is proportional to the electric field squared.

Integration spaces are used to calculate the maximum and average normal electric fields near the edge of the nanostructure. For Figure 3, these rectangular integration spaces (not shown) are designed to be 10 nm wide and twice the size of the height, and they are centered on the edge of the nanowire cross section. For all of the simulations of Figure 3, the height of the space was kept constant so that the integration space can be taken as a constant area. As the device geometry changes, the integration space was designed to move with the edge so that it consistently calculates the enhancement on the same relative position of the device.

Figure 3c plots the average enhancement in this integration space as a function of width, w_{L}, and incident wavelength. The color of each pixel of Figure 3c represents the average enhancement in the integration space for a model with a specific width and wavelength combination. The color scale is shown in Figure 3c. The results show that the widths that give the greatest enhancement for specific wavelength have a linear relationship as a function of wavelength.

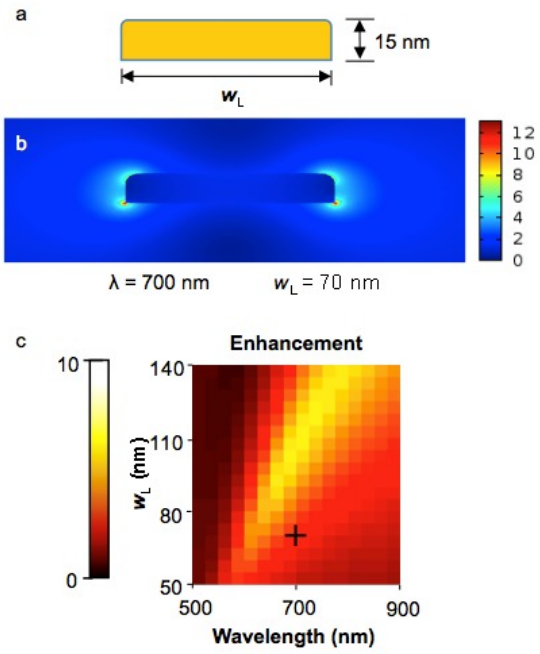

Figure 3. Computational model of an infinitely long nanowire with a rectangular cross section with beveled top corners. The simulation varied the nanowire width, w_L and the wavelength of the incident light. (a) Simulation cross-sectional nanowire geometry with width, w_L, and height of 15 nm. (b) Calculated electric field distribution for w_L = 70 nm and a wavelength of 700 nm as a function of position around the nanowire. (c) The average enhanced electric field, E_{local}/E_0, near the nanowire edge as a function of width and wavelength. The cross on plot represents the structure and wavelength combination in (b).

A second set of models was created to simulate the effects of the optical plasmonic nanogap (Figure 4). These models consist of two infinitely long rectangles of width 140 nm separated by a nanogap. Both rectangles have 5 nm radius fillets on the top corners, and are 15 nm tall. The simulation was made to sweep through different gap widths from 1 to 50 nm and plots the optical gain versus this gap thickness, as shown in Figure 4. The gain or enhancement is equal to the EFD squared. The wavelength was kept constant for this model at 875 nm and the incident light polarization was transverse to the nanowire width with the electric field vector pointing across the gap.

The geometry of the device is built in the center of a circular 2D simulation space. This circle is comprised of two layers: the perfectly matched layer (PML) and the far field domain. The far field domain is the inner layer of the circle with a radius of 800 nm. This space, the environment through which the incident electromagnetic wave propagates before and after it interacts with the device, is filled with the material parameters of air with an effective medium of n_{eff} =1.25. This approximates substrate effects the geometry of which is not included in the model, similar to prior work.[3] The resulting scattered or transmitted light then propagates towards the outer boundary of the far field domain. At this point, the PML absorbs the electromagnetic radiation. The PML is a 300 nm thick layer of the circle that begins where the far field domain ends. The purpose of this is to absorb the light that has already interacted with the device so that it will not scatter back into the simulation space. This provides a truncation point for the computational region and reduces noise, producing accurate results. The insets of Figure 4 show the nanogap region for some of these models with the enhancement plotted with a jet color scale.

The gap between two infinitely long nanowires of constant width was shown to have a noticeable effect on the optical enhancement within the gap. This set of models clearly shows strong enhancement and optical gain in the nanogap, and it shows that this optical gain, $(E_{local}/E_0)^2$, increases significantly as the gap size decreases. As the gap width was decreased from 50 nm to 10 nm, the enhancement was found to increase at a nearly linear rate. From gap widths of 10 to 1 nm, the optical enhancement was shown to increase at closer to an exponential rate. These data are plotted in Fig. 3 along with COMSOL electric field enhancement results for gaps of width 1, 5, 10, 25, and 50 nm.

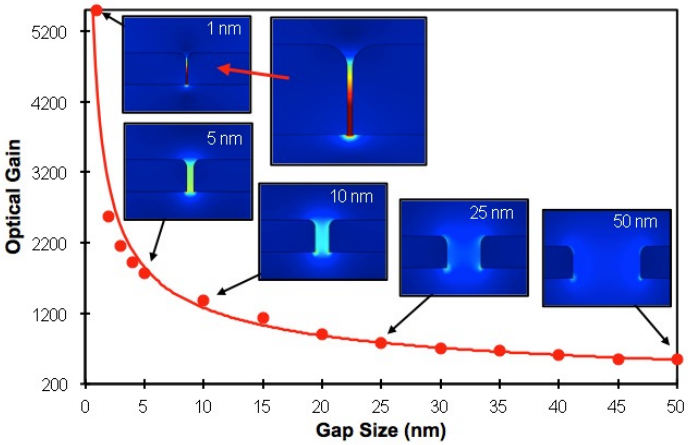

Figure 4. Simulation of two infinitely long rectangular nanowires of 140 nm width with a constant incident wavelength of 875 nm, with varying gap size. The optical gain (or enhancement), $(E_{local}/E_0)^2$, is plotted as a function of gap size. Insets show cross-section of gap region with the enhanced electric field distribution shown with color variation for nanogaps of 1, 5, 10, 25, 50 nm.

5. CONCLUSIONS

This work has successfully implemented the self-aligned technique to fabricate large area arrays of mass-producible nanostructures. This proves yet again the versatility and transferability of the self-aligned technique. These are preliminary results and many more structures will be fabricated with various geometries in the near future. Additionally, preliminary computational electromagnetic models have been created to help optimize the device geometry for maximum enhancement and plasmonic applications. Moreover, a preliminary nanogap simulation has shown the significance of the gap and how the optical gain and enhancement in the gap increase exponentially as the gap size decreases. Therefore, the self-aligned technique is critical to fabricating plasmonic structures with maximum enhancements. This will improve the quality of plasmonic devices and lead to future plasmonic applications or commercial products.

ACKNOWLEDGEMENTS

We would like to acknowledge the following colleagues at the University of Arkansas for all of their help and support: Yahia Makableh & Dr. O. Manasreh, Mourad Benamara, Dick Penhallegon, Brandon Rogers, Rob Sleezer, and Dr. William Oliver III. I would also like to thank Joe Nabity for his technical support with NPGS. Funding for this research has been provided by the Department of Physics, the Fulbright College of Arts and Sciences, and the Vice Provost for Research and Economic Development at the University of Arkansas. Stephen J. Bauman has been supported by the Doctoral Academy Fellowship through the University of Arkansas Graduate School, and travel funding for this presentation has been provided by the SPIE student travel grant, and the University of Arkansas Graduate School travel grant.

REFERENCES

[1] Walsh, G. F.., Negro, L. D., “Engineering Plasmon-Enhanced Au Light Emission with Planar Arrays of Nanoparticles,” Nano Lett. **13**(2), 786–792 (2013).

[2] Natelson, D., Li, Y.., Herzog, J. B., “Nanogap structures: combining enhanced Raman spectroscopy and electronic transport,” Phys. Chem. Chem. Phys. **15**(15), 5262–5275 (2013).

[3] Herzog, J. B., Knight, M. W., Li, Y., Evans, K. M., Halas, N. J.., Natelson, D., "Dark Plasmons in Hot Spot Generation and Polarization in Interelectrode Nanoscale Junctions," Nano Lett. **13**(3), 1359–1364 (2013).
[4] Atwater, H. A.., Polman, A., "Plasmonics for improved photovoltaic devices," Nat. Mater. **9**(3), 205–213 (2010).
[5] Mukherjee, S., Sobhani, H., Lassiter, J. B., Bardhan, R., Nordlander, P.., Halas, N. J., "Fanoshells: Nanoparticles with Built-in Fano Resonances," Nano Lett. **10**(7), 2694–2701 (2010).
[6] Yang, Z.-J., Kim, N.-C., Li, J.-B., Cheng, M.-T., Liu, S.-D., Hao, Z.-H.., Wang, Q.-Q., "Surface plasmons amplifications in single Ag nanoring," Opt. Express **18**(5), 4006–4011 (2010).
[7] Stockman, M. I., "Nanoplasmonics: The physics behind the applications," Phys. Today **64**(2), 39–44 (2011).
[8] Ding, P., He, J., Wang, J., Fan, C., Cai, G.., Liang, E., "Low-threshold surface plasmon amplification from a gain-assisted core–shell nanoparticle with broken symmetry," J. Opt. **15**(10), 105001 (2013).
[9] Huang, Y.-W., Chen, W. T., Wu, P. C., Fedotov, V. A., Zheludev, N. I.., Tsai, D. P., "Toroidal Lasing Spaser," Sci. Rep. **3** (2013).
[10] Herzog, J. B., Knight, M. W.., Natelson, D., "Thermoplasmonics: Quantifying Plasmonic Heating in Single Nanowires," Nano Lett. **14**(2), 499–503 (2014).
[11] Baffou, G.., Quidant, R., "Thermo-plasmonics: using metallic nanostructures as nano-sources of heat," Laser Photonics Rev. **7**(2), 171–187 (2013).
[12] Rodríguez-Oliveros, R.., Sánchez-Gil, J. A., "Gold nanostars as thermoplasmonic nanoparticles for optical heating," Opt. Express **20**(1), 621–626 (2012).
[13] Chang, T. H. P., "Proximity effect in electron-beam lithography," J. Vac. Sci. Technol. **12**(6), 1271–1275 (1975).
[14] Fursina, A., Lee, S., Sofin, R. G. S., Shvets, I. V.., Natelson, D., "Nanogaps with very large aspect ratios for electrical measurements," Appl. Phys. Lett. **92**(11), 113102 (2008).
[15] Zhu, W., Banaee, M. G., Wang, D., Chu, Y.., Crozier, K. B., "Lithographically Fabricated Optical Antennas with Gaps Well Below 10 nm," Small **7**(13), 1761–1766 (2011).
[16] Scholder, O., Jefimovs, K., Shorubalko, I., Hafner, C., Sennhauser, U.., Bona, G.-L., "Helium focused ion beam fabricated plasmonic antennas with sub-5 nm gaps," Nanotechnology **24**(39), 395301 (2013).
[17] Xu, Q., Bao, J., Rioux, R. M., Perez-Castillejos, R., Capasso, F.., Whitesides, G. M., "Fabrication of Large-Area Patterned Nanostructures for Optical Applications by Nanoskiving," Nano Lett. **7**(9), 2800–2805 (2007).